



**The 14<sup>th</sup> ISAV2024**  
**International Conference on**  
**Acoustics and Vibration**  
11-12 Dec 2024      Karaj - Iran



# Accurate Crack Length Estimation in steel plate by Integrating ABAQUS Simulation and Phased Array Acoustic Waves

*Elahe Sarlakian<sup>a</sup>, Aghil Yousefi-Koma<sup>a\*</sup>, Nazanin Barzin<sup>a</sup>,  
Ehsan Ghafarollahi<sup>a</sup>*

*<sup>a</sup> Center of Advanced Systems and Technologies, School of Mechanical Engineering,  
University of Tehran, 11155-4563, Tehran, Iran.*

*\* Corresponding author e-mail: [aykoma@ut.ac.ir](mailto:aykoma@ut.ac.ir)*

## Abstract

This study investigates the estimation of crack lengths in steel plates using ABAQUS simulations and acoustic analysis through the Pressure of Reflection (PoR) and phased array techniques. An oblique crack at a 45-degree angle is defined in ABAQUS with a fine mesh of 0.002 for high-resolution results, employing the explicit library and the acoustic element family. Acoustic pressure data are extracted and averaged across selected nodes, focusing on significant readings. A pressure threshold of 0.003 Pa identifies high-amplitude readings, allowing extraction of timestamps for the first and last significant peaks. Crack length is estimated by calculating the time interval between these pressure points and multiplying it by the speed of longitudinal sound, derived from the material's bulk modulus and density. Fast Fourier Transform (FFT) is used to convert time-domain pressure data into the frequency domain, identifying dominant frequencies for crack lengths ranging from 1 cm to 28 cm. Peak frequencies are plotted to illustrate their relationship with crack dimensions, highlighting the influence of crack size on acoustic responses. The comparison of actual and measured crack lengths yielded a Root Mean Square Error (RMSE) of 0.0797 and an average error of 1.1216%, indicating a high degree of accuracy. This research demonstrates the effectiveness of using PoR and phased array methods for optimal wave interactions with cracks, showcasing the potential of acoustic techniques in assessing structural integrity for non-destructive testing.

**Keywords:** crack length estimation; ABAQUS simulations; acoustic analysis; phased array techniques.

---

## 1. Introduction

Structural integrity is essential in aerospace, civil, and mechanical engineering, as cracks can lead to severe failures. Cawley and Adams (1979) demonstrated the effectiveness of ultrasonic techniques for crack detection, emphasizing their importance in ensuring safety [1].

Liu, Zhang, and Chen (2017) integrated finite element analysis (FEA) with acoustic emission to improve crack detection and monitoring in composite materials [2].

Meyer and O'Donnell (1995) highlighted the advantages of phased array techniques, which enhance defect detection capabilities [3]. Tan and Lee (2014) showcased FEA's role in simulating wave interactions with cracks, providing valuable insights into crack behavior [4]. Boller and Fuchs (2009) emphasized the significance of structural health monitoring, linking theoretical concepts to practical applications in engineering [5].

Recent advancements in machine learning have further enhanced detection accuracy, as noted by Zhang, Wang, and Wu (2020), who reviewed its applications in structural monitoring [6]. Additionally, Khan and Sinha (2019) focused on using advanced signal processing methods, such as FFT, for improved crack characterization [7]. Zhang and Chen (2018) provided a comprehensive review of fracture mechanics and its applications in structural health monitoring, underscoring the need for robust methodologies [8].

## 2. Theory

The assessment of crack lengths in steel components via acoustic methods relies on wave propagation and signal processing. Acoustic waves reflect and undergo mode conversion when encountering a crack, revealing critical characteristics. This simulation models piezoelectric effects through acoustic pressure and employs FEA in ABAQUS to simulate longitudinal wave propagation in a steel plate. Signal analysis utilizes FFT to convert time-domain data to the frequency domain, enabling identification of dominant frequencies associated with varying crack lengths and enhancing material integrity assessment in non-destructive testing.

### 2.1 Acoustic wave propagation

The speed of longitudinal waves  $c_L$  was calculated using the formula:

$$c_L = \sqrt{\frac{K}{\rho}} \quad (1)$$

Where  $c_L$  is the speed of longitudinal sound in the material,  $K$  is the bulk modulus that measures the material's resistance to uniform compression, and  $\rho$  is the density of the plate.

### 2.2 Time delay calculation

The speed of longitudinal sound informed the time delays for the phased array elements, calculated using the formula:

$$\Delta t_n = \frac{n \times l \times \sin(\theta)}{c_L} \quad (2)$$

Where  $n$  represents the index of the element,  $l$  is the center-to-center distance between adjacent elements,  $\theta$  is the desired steering angle of the acoustic beam, and  $c_L$  is the speed of sound in steel.

### 2.3 Crack length calculation

Crack length estimation is achieved by analyzing high-amplitude pressure readings, with a threshold set to identify significant peak frequencies. The timestamps of these peaks are used to calculate the time interval between the first and last peaks. The crack length is then estimated using the formula:

$$\text{Crack length} = c_L \cdot \text{time interval} \quad (3)$$

Where  $c_L$  is the speed of longitudinal sound.

## 2.4 Root Mean Square Error (RMSE)

RMSE is a metric that quantifies the discrepancies between real values and calculated values. It is calculated using the formula:

$$\text{RMSE} = \sqrt{\frac{1}{n} \sum_{i=1}^n (y_i - \hat{y}_i)^2} \quad (4)$$

Where  $y_i$  represents the real values,  $\hat{y}_i$  represents the calculated values, and  $n$  is the number of the data points.

## 3. Method

### 3.1 Simulation

In the simulation, a  $0.5\text{m} \times 0.5\text{m}$  steel plate was modeled with a bulk modulus of  $1.75 \times 10^{11}$  Pa and a density of  $7800 \text{ kg/m}^3$ . FEA was conducted using Abaqus, employing the explicit library and the acoustic element family to model the material behavior under acoustic excitation. As illustrated in Figure 1, The crack was represented as a line at a 45-degree angle to the horizontal. To accurately characterize the crack, the seam feature was utilized in the interaction module. A mesh size of  $0.002 \text{ m}$  was applied to ensure sufficient resolution for the subsequent acoustic analysis.

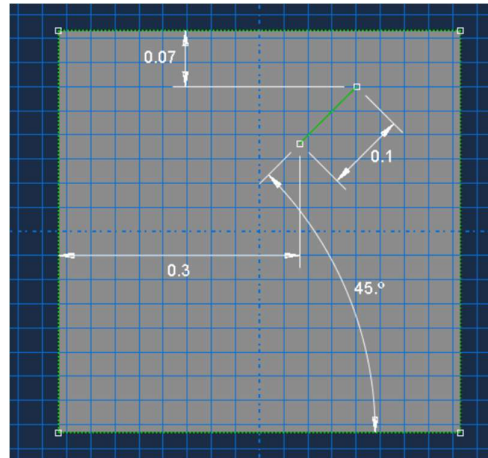
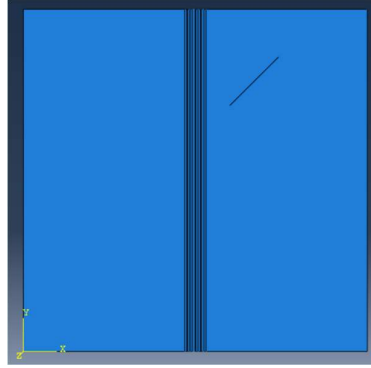


Figure 1. Dimensions of the line-shaped crack in the steel plate (dimensions in meters).

As shown in Figure 2, An eight-element phased array system, with each element measuring  $3 \text{ mm}$  wide and  $1 \text{ mm}$  apart, generated longitudinal acoustic waves directed at a crack using specific time delays for optimal interaction.



**Figure 2.** Steel plate with a 45-degree crack and sensor element arrangement.

Each of the elements also functioned as a pressure sensor to record the reflected waves after they interacted with the crack.

As shown in Figure 3, reflected acoustic waves interact with the crack in the steel plate, displaying the POR distribution. Warmer colors indicate higher pressure levels, highlighting the crack's impact on wave behavior and material integrity.

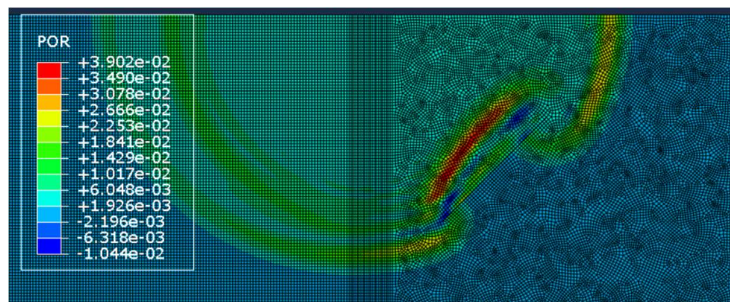


**Figure 3.** reflected acoustic waves after interacting with the crack.

### 3.2 Data collection

The crack length in the steel plate varies from 1 cm to 28 cm, generating new mesh configurations for optimal resolution in the FEA in ABAQUS. After running the simulation, individual pressure-time plots are averaged to clarify acoustic wave behavior. The average acoustic pressure, or POR, is calculated for selected nodes, resulting in a dataset of pressure (Pascals) and time (seconds) exported to an Excel file in CSV format for further analysis of the relationship between crack length and acoustic response.

### 3.3 Data preprocessing

The pressure-time plot from ABAQUS spans 0 to 15e-05 seconds, capturing the acoustic signal's response. In signal processing, extraneous segments, such as transmitted waves, are removed for clarity. The maximum pressure point, indicating peak interaction with the crack, is identified, and subsequent data points are eliminated to reduce noise. This focus on data up to the peak enhances insights into structural defects, ensuring robust and meaningful results for further evaluations.

### 3.4 Signal processing

Pressure-time data from ABAQUS simulations was analyzed using FFT to identify dominant frequencies related to crack lengths. This involved loading data from a CSV file into a Pandas DataFrame and applying FFT using the NumPy library to calculate frequency components.

### 3.5 Crack length estimation

The CSV file imported into a Jupyter Notebook for the crack length estimation. A pressure threshold of 0.003 Pa was set to identify peak frequencies associated with the crack, focusing on readings above this value. The analysis extracted timestamps for these high-amplitude pressure points, allowing the calculation of the time interval between the first and last peaks.

The crack length was then estimated by multiplying this time interval by the speed of sound.

## 4. Results

### 4.1 Time delay calculation

As depicted in Figure 4, the time delay calculation resulted in a linear increase in time delay from element 1 to element 8, effectively generating discrete points in the emission of signals to steer the acoustic wave towards the desired angle. This linear increment of time delays enabled the phased array to accurately focus and direct the longitudinal acoustic waves towards the crack.

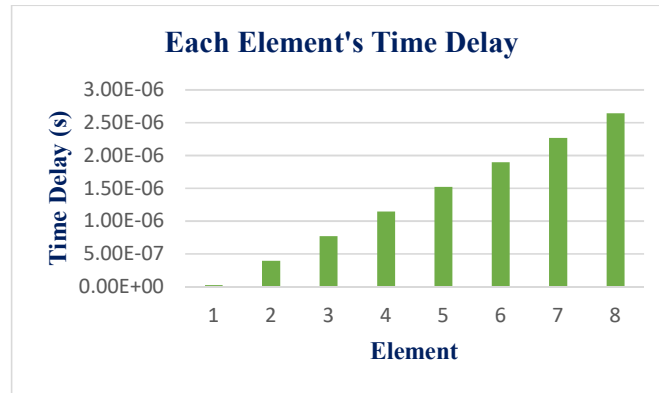


Figure 4. Linearly increase of time delay.

### 4.2 Pressure-time plot analysis

Figure 5 displays individual pressure-time responses from multiple sensors, showing variations in acoustic pressure as the crack length changes. Due to the complexity and noise in these individual plots, averaging the data provides a clearer representation of the overall acoustic wave behavior. This approach enhances the reliability of measurements used to assess the relationship between crack length and acoustic response.

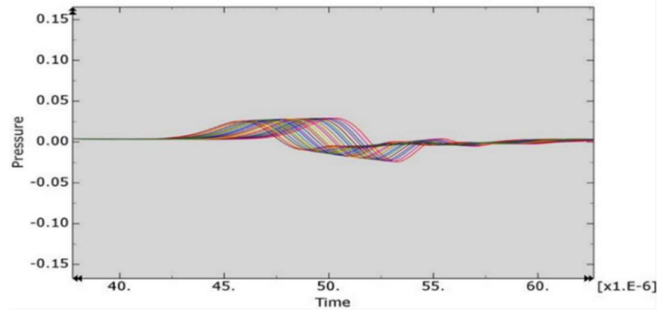


Figure 5. Individual sensors' pressure-time plots

As presented in Figure 6, the acoustic pressure-time plot for a 15 cm crack shows an initial sharp peak from the acoustic wave, followed by diminishing oscillations and a notable secondary peak around  $6.9 \times 10^{-5}$  seconds, indicating interaction with the crack. The pressure then stabilizes near zero, reflecting minimal ongoing activity.

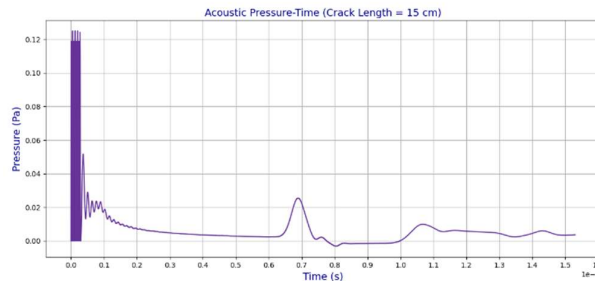


Figure 6. Acoustic pressure VS time plot (average sensors' pressure-time data)

### 4.3 Frequency Domain Response of Acoustic Pressure

Figure 7 illustrates the frequency domain response derived from the pressure-time data. The x-axis represents frequency (Hz), while the y-axis indicates magnitude. The curve exhibits a high magnitude at lower frequencies, which gradually declines, suggesting a stronger acoustic response in the lower frequency range. This analysis is crucial for identifying significant frequencies associated with crack interactions, thereby enhancing the understanding of the material's condition.

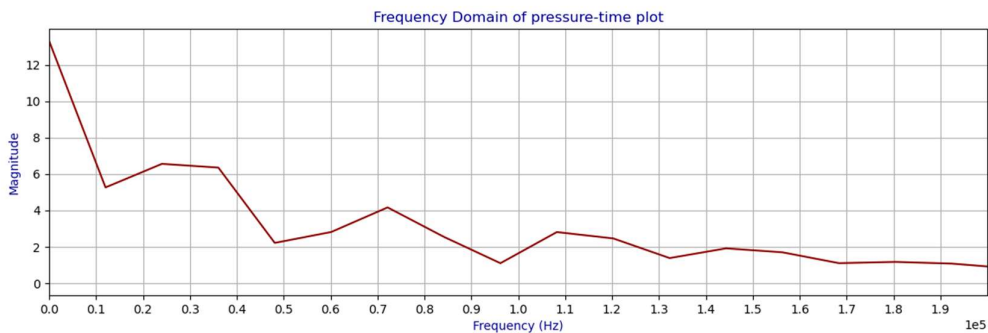


Figure 7. Transformation of pressure-time data to the frequency domain.

### 4.4 Dominant peaks determination

Peaks in the frequency spectrum were identified using the `find_peaks` function with a prominence threshold. Frequency and time indices were compiled into a DataFrame. The

analysis of crack lengths from 1 cm to 28 cm resulted in a scatter plot, as shown in Figure 8(a), illustrating the relationship between frequency and crack length. This highlights the significance of frequency analysis for structural integrity and non-destructive testing.

The line plot as shown in Figure 8(b), illustrates the linear increase in peak frequency over time for crack lengths of 5 cm, 15 cm, 25 cm, and 28 cm. The consistent rise indicates changes in material properties or wave propagation, offering insights for monitoring structural integrity.

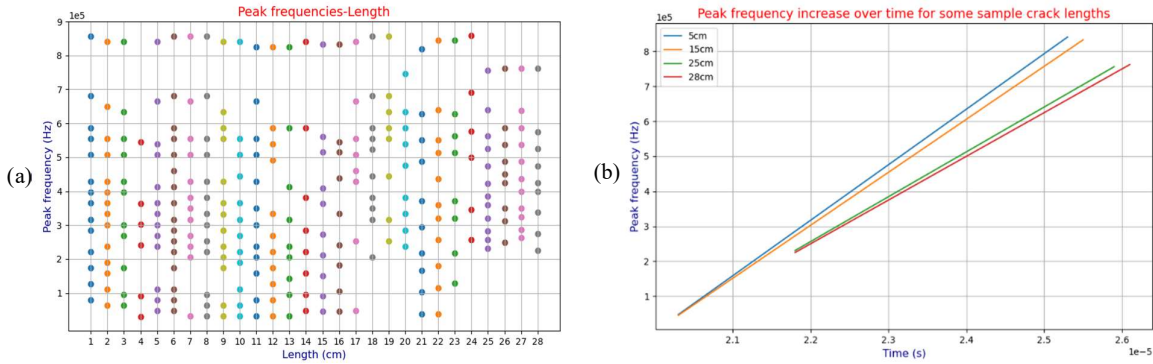


**Figure 8.** High amplitude frequency range for each crack length (a); Peak frequency increase over time (b).

#### 4.5 Comparison of actual and estimated crack length

Figure 9 illustrates the pressure-time plot after preprocessing for a real crack length of 23 cm and an estimated length of 23.0914 cm. It highlights high-amplitude pressure readings above a threshold, indicating significant acoustic interactions, and is used to determine time intervals between dominant peaks for crack assessment.

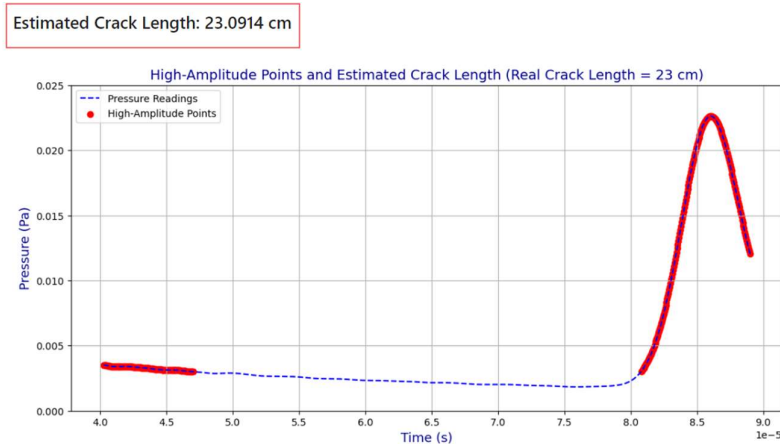


**Figure 9.** An example of Crack length estimation using high-amplitude points.

Table 1 compares real and estimated crack lengths in centimeters. The first column lists actual lengths, while the second shows estimated values. This comparison highlights the accuracy of the estimation method across various crack lengths.

Table 1. Sample comparison of real and estimated crack lengths (cm).

Real Length (cm)	Estimated Length (cm)
1.0000	1.1368
2.0000	1.9657
3.0000	3.0788
4.0000	4.0262
5.0000	4.9753
6.0000	6.1120
7.0000	7.0340
8.0000	8.1471
9.0000	9.0708
10.0000	10.0892
11.0000	11.0365
12.0000	12.0865
13.0000	13.0702
14.0000	13.9732
15.0000	14.9206
16.0000	16.0574
17.0000	17.0521
18.0000	18.0231
19.0000	18.9468
20.0000	19.8941
21.0000	21.1020
22.0000	21.9783
23.0000	23.0914
24.0000	24.1571
25.0000	25.1045
26.0000	26.0518
27.0000	26.9992
28.0000	27.9465

## 5. Conclusion

This study integrates FEA with acoustic wave modeling to enhance crack detection and length estimation in steel plates. Although direct piezoelectric effects were not simulated, their influence was effectively represented through acoustic pressure. By modeling longitudinal wave propagation in ABAQUS and analyzing pressure-time graphs, peak pressure points were correlated with crack reflections. The time interval between these peaks facilitated the determination of crack length using the speed of sound as a multiplier. The comparison of actual and measured crack lengths yielded an RMSE of 0.0797 and an average error of 1.1216%, indicating a high degree of accuracy. This research underscores the efficacy of phased array techniques in non-destructive evaluation and structural health monitoring.

## REFERENCES

1. P. Cawley, & R. D. Adams, The location of defects in structures using ultrasonic techniques. *Journal of Sound and Vibration*, 64(2), 189-197 (1979).
2. Y. Liu, J. Zhang, & Y. Chen, Crack detection and monitoring in composite materials using acoustic emission and finite element analysis. *Composites Part B: Engineering*, 113, 193-203 (2017).
3. A. Meyer, & M. O'Donnell, The use of phased array ultrasonic techniques for crack detection. In *Advances in Nondestructive Testing and Evaluation* 135-142. Springer (1995).
4. D. Tan, & K. Lee, Finite element modeling of crack propagation in elastic materials. *International Journal of Solids and Structures*, 51(1), 36-47 (2014).
5. C. Boller, & H. Fuchs, *Structural Health Monitoring: A New Approach to Measuring the Integrity of Structures*. Springer (2009).
6. Y. Zhang, W. Wang, & Y. Wu, Machine learning for crack detection in structures: A review. *Computers in Industry*, 113, 103128 (2020).
7. M. I.Khan, & A. K. Sinha. Acoustic emission-based crack size estimation using wavelet transform. *Materials Today: Proceedings*, 18, 2331-2336, (2019).
8. W. Zhang, & L. Chen, A comprehensive review of fracture mechanics and its applications in structural health monitoring. *Engineering Structures*, 171, 118-131 (2018).